Diagnosing and Correcting Systematic Errors in Spectral-Based Digital Imaging

Mahnaz Mohammadi and Roy S. Berns, Munsell Color Science Laboratory, Chester F. Carlson Center for Imaging Science, Rochester Institute of Technology, Rochester, New York, USA

Abstract

A digital imaging system containing a calibration target, an image capture device, and a mathematical model to estimate spectral reflectance factor was treated as a spectrophotometer and as such subject to systematic and random errors. The systematic errors considered were photometric zero, photometric linear and nonlinear scale, wavelength linear and nonlinear scale, and bandwidth. To diagnose and correct the systematic errors in a spectral imaging system, a technique using multiple linear regression as a function of wavelength was employed, based on the measurement and image based estimating of several image verification targets. Based on the stepwise regression technique, the most significant diagnosed systematic errors were photometric zeros, photometric linear scale, wavelength linear scale, and bandwidth errors. The performance of spectral imaging after correction of the estimated spectral reflectance, based on the modeling result, was improved on average 25.3% spectrally and 16.7% colorimetrically. This technique is suggested as a general method to improve the performance of spectral imaging systems.

Introduction

The accuracy of a spectral imaging system is dependent upon several parameters including the image capture device, the calibration target, and the mathematical method to estimate spectral reflectance factor. Since the total system generates spectral reflectance factor, the errors associated with conventional spectrophotometry can be considered for spectral imaging. Spectrophotometric errors can be divided into systematic and random errors. Systematic errors include errors resulting from wavelength, bandwidth, detector linearity, nonstandard geometry, and polarization.[1,2] Totally, systematic errors are caused by characteristics of the instrument that are the same for all measurements. Measurement of systematic errors is the evaluation of accuracy of the measurements. Random errors are caused by inability to control the instrument. That might be caused from drift, electronic noise, and sample presentation. But it is not limited to these error sources. Random errors, by definition, are discussed in terms of probabilities. A standard deviation indicates the probability of the existence of random error. Based on error propagation theory,[3] the random errors can propagate through several steps of a calibration process and finally can be a parameter to calculate systematic error. Hence, it is not true to say that the accuracy of a spectrophotometer is affected just by the systematic errors.

Berns and Petersen[2] have developed a technique based on the use of multiple linear regression to model systematic spectrophotometric errors and subsequently correct spectral measurements based on the modeling result. The developed technique is currently used in industrial environments. Berns' method was first described by Robertson,[4] who demonstrated its utility in diagnosing photometric zero and linear photometric scale errors in a General Electric Recording Spectrophotometer.

To improve the instrument performance, the first step is to diagnosis the errors and the second step is to correct an instrument's systematic errors. To determine which error parameters are statistically significant, stepwise regression[5] was suggested.

In this research, it was presumed that a combination of a calibration target, image capture device, and the mathematical model to estimate spectral reflectance factor was equivalent to a typical spectrophotometer. The systematic errors, including photometric zero, photometric linear and nonlinear scale, wavelength linear and nonlinear scale and bandwidth were considered as the possible errors in the spectral imaging system. The systematic errors were modeled by a series of equations and minimized using the multiple linear regression technique. It was assumed that the random errors were negligible.

Calibration and Verification Targets

A set of common targets included the GretagMacbeth ColorChecker Color Rendition Chart (CC), the GretagMacbeth ColorChecker DC (CCDC), and the Esser TE221 scanner Test Chart (Esser) along with two targets containing typical artist's paints using Gamblin Conservation Colors were used as targets to both diagnose and correct the systematic errors in a spectral imaging system. The Gamblin and EXP target contain 63 and 14 colors, respectively. The EXP target[6-9] was developed based on analysis the Gamblin Conservation Colors using Kubelka-Munk[10] turbid media theory. All the targets were measured using a GretagMacbeth Color XTH, integrating sphere specular component excluded in the wavelength range of 360 to 750 nm in intervals of 10 nm with a small aperture. The instrument was the reference spectrophotometer and by definition, assumed to be error-free.

Spectral Image Acquisition

Images of the targets and a uniform grey background were captured using a modified Sinarback 54 digital camera in its ″four-shot″ mode. The Sinarback 54 is a three channel digital camera that incorporates a Kodak KAF-22000CE CCD with a resolution of 5440×4880 pixels. This camera has been modified[11] by replacing its IR cut-off filter with clear glass and fabricating two filters used sequentially, resulting in a pair of RGB images. For this experiment, a pair of Elinchrom Scanlite 1000 tungsten lights was used, producing a correlated color temperature of 2910 K. All images were digitally flat fielded using the grey background followed by image registration.

Spectral reflectance factor was estimated from linear photometric camera signals by a matrix transformation:

$$\hat{\mathbf{R}} = \mathbf{T} \Diamond \mathbf{D} \tag{1}$$

where $\hat{\mathbf{R}}$ is the vector of estimated reflectance factors, $\mathbf{D}$ is a digital count vector, and $\mathbf{T}$ is the transformation matrix. The transformation matrix was derived using the measured spectral reflectance factors and the captured digital counts for each calibration target. A SVD-based pseudo inverse technique was used to derive the transformation matrix.

Mathematical Description of Systematic Errors

The method is based on the use of multiple linear regression to diagnose and correct systematic errors. These errors are photometric zero, photometric linear and nonlinear scale, wavelength linear and nonlinear scale, and bandwidth. A brief definition of the mentioned systematic errors is as follows:

Photometric Zero Error

The error incurred by ambient light is called photometric zero error. In addition, the stray light associated with input optics, the use of a black trap with the finite reflectance factor, or ignoring detector dark current might be further sources of photometric zero errors in spectrophotometric measurements. The offset of the entire photometric scale is defined as the photometric zero error and expressed as

$$R_t(\lambda) = R_e(\lambda) + \beta_0 \tag{2}$$

where $R_t(\lambda)$ and $R_e(\lambda)$ are true and estimated reflectance factor, and β_o is the photometric zero error. In the current model, the true reflectance factor is assumed to be the reflectance factor measured by the spectrophotometer and the estimated reflectance factor is that estimated using the imaging system.

Photometric Linear Scale Error

An improper white standard can cause this error, in which the upper portion of the photometric scale is more affected than the lower portion. This error is called photometric linear error and is expressed mathematically as

$$R_t(\lambda) = R_e(\lambda) + \beta_1 R_e(\lambda) \tag{3}$$

where β_1 is the photometric scale error.

Photometric Nonlinear Scale Error

The detector nonlinearity causes a photometric nonlinear scale error. A nonlinear weighting function approximates this systematic error, expressed as

$$R_t(\lambda) = R_e(\lambda) + \beta_2 \left[1 - R_e(\lambda)\right] R_e(\lambda) \tag{4}$$

where β_2 is the photometric nonlinear scale error.

Wavelength Scale Error

A shift in the wavelength scale due to mechanical problems causes a wavelength scale error. In spectrophotometric measurements, the resulting error in reflectance factor is approximately proportional to the first derivative of the measured reflectance factor. This error might be linear or nonlinear with respect to wavelength. The wavelength linear and nonlinear scale errors are expressed mathematically as

$$\begin{aligned} R_t(\lambda) &= R_e(\lambda) + \beta_3\, dR_e/d\lambda \\ R_t(\lambda) &= R_e(\lambda) + \beta_4 w_1\, dR_e/d\lambda \\ w_1(\lambda) &= \frac{\lambda - \lambda_{first}}{\lambda_{last} - \lambda_{first}} \left(1 - \frac{\lambda - \lambda_{first}}{\lambda_{last} - \lambda_{first}}\right) \\ R_t(\lambda) &= R_e(\lambda) + \beta_5 w_2\, dR_e/d\lambda \\ w_2(\lambda) &= \sin 2\pi(\lambda/200) \end{aligned} \tag{5}$$

where β_3, is wavelength linear scale error and β_4 and β_5 are examples of wavelength nonlinear scale errors, which Berns[2] proposed for the spectrophotometer employed in his research. The wavelength nonlinear scale error would be varied for different instruments. The quadratic wavelength nonlinear scale error is more general than the other one. The $dR_e/d\lambda$ is the first derivative of the estimated reflectance with respect to wavelength, and equal to,

$$(dR/d\lambda)_i = \frac{R(\lambda_{i+1}) - R(\lambda_{i-1})}{(\lambda_{i+1}) - (\lambda_{i-1})} \tag{6}$$

where i is an index of wavelength.

Bandwidth Error

Variation of the spectral bandwidth with wavelength in a photometric instrument causes an error in the measured reflectance factor. The bandwidth scale error is approximately proportional to the second derivative of the measured reflectance factor with respect to wavelength. It is expressed as

$$R_t(\lambda) = R_e(\lambda) + \beta_6\, d^2R_e/d\lambda^2 \tag{7}$$

where β_6 is bandwidth error and $d^2R_e/d\lambda^2$ is the second derivative of $R_e(\lambda)$ with respect to wavelength, equal to

$$(d^2R/d\lambda^2)_i = \frac{R(\lambda_{i+1}) + R(\lambda_{i-1}) - 2R(\lambda_i)}{\left(\frac{\lambda_{i+1} - \lambda_{i-1}}{2}\right)^2} \tag{8}$$

Regression Model

The systematic spectrophotometric errors along with their model definitions are tabulated in Table 1.

Table 1: The Systematic Errors and Their Modeled Equations, Including Their Notation and the Notation of the Parameters

Systematic Error	Parameter	Model
Photometric zero	$\beta 0$	$X_0(\lambda)=1$
Photometric linear scale	$\beta 1$	$X_1(\lambda)=R_e(\lambda)$
Photometric nonlinear scale	$\beta 2$	$X_2(\lambda)=[1-R_e(\lambda)]R_e(\lambda)$
Wavelength linear scale	$\beta 3$	$X_3(\lambda)=dR_e/d\lambda$
Wavelength nonlinear scale (quadratic)	$\beta 4$	$X_4(\lambda)=w_1(\lambda)dR_e/d\lambda$
Wavelength nonlinear scale (sine wave)	$\beta 5$	$X_5(\lambda)=w_2(\lambda)dR_e/d\lambda$
Bandwidth	$\beta 6$	$X_6(\lambda)=d^2R_e/d\lambda^2$

Suppose that all seven systematic errors occur in the imaging system. The difference between the estimated and true reflectance factor is expressed as

$$R_t(\lambda)-R_e(\lambda)=\beta_0X_0(\lambda)+\beta_1X_1(\lambda)+...+\beta_6X_6(\lambda)+e(\lambda) \quad (9)$$

where β_0, β_1,…, β_6 are the weighting parameters of each systematic error and $e(\lambda)$ is the residual error not accounted by the model. In order to characterize the wavelength errors comprehensively, the regression technique was extended to generate regression coefficients as a function of wavelength. Equation 9 can be rewritten as

$$R_t(\lambda)-R_e(\lambda)=\beta_0(\lambda)X_0(\lambda)+...+\beta_6(\lambda)X_6(\lambda)+e(\lambda) \quad (10)$$

The vector-matrix form of Eq. 10 is

$$\mathbf{Y}_i=\mathbf{X}_i\mathbf{B}_i+\mathbf{e} \quad (11)$$

where

$$\mathbf{X}_{\lambda=i}=\begin{bmatrix} X_{01}. & . & .X_{m1} \\ . & & \\ . & & \\ . & & \\ X_{0n}. & . & .X_{mn} \end{bmatrix}, \quad \mathbf{B}_i=\begin{bmatrix}\beta_0\\ .\\ .\\ .\\ \beta_m\end{bmatrix} \quad (12)$$

$$\mathbf{Y}_{\lambda=i}=\begin{bmatrix}(R_t-R_e)_1\\ .\\ .\\ .\\ (R_t-R_e)_n\end{bmatrix}, \quad \mathbf{e}_{\lambda=i}=\begin{bmatrix}e_1\\ .\\ .\\ .\\ e_n\end{bmatrix}$$

where n is the number of samples in the target, m is the selected error parameters and i is a single wavelength. The regression was performed to estimate the elements in **B**; the process was repeated for each estimated wavelength. The magnitudes of the regression coefficients β_0,β_1,…, β_m indicate the magnitudes of the corresponding systematic errors at a single wavelength for the imaging system.

The estimated reflectance factor can be corrected by the regression coefficients as

$$R_c(\lambda)=R_e(\lambda)+\beta_0(\lambda)X_0(\lambda)+...+\beta_6(\lambda)X_6(\lambda) \quad (13)$$

where $R_c(\lambda)$ is the corrected reflectance factor. The above regression model has been developed to correct the systematic errors.

Based on the model described in Table I, the errors are functions of the estimated reflectance factor. To diagnose the systematic error, the Robertson method[3] was employed. In Robertson's research, the errors described by linear equations were functions of the true data, $R_T(\lambda)$. The advantage of this method is that the magnitude of the coefficients β_0, β_1,…, β_6 directly describe systematic errors.

Results and Discussion

The effectiveness of the technique was tested to diagnose and correct the systematic errors of an imaging system. A SVD-based pseudoinverse technique was used to derive the transformation matrix for converting captured digital counts to spectral reflectance factor. The measured reflectance factor using the Color XTH spectrophotometer was assumed to be the true reflectance factor and the estimated one was that corrected by the regression method. Several targets described in part II were employed as imaging system calibration and spectrophotometric diagnostic and correction targets.

To diagnose the systematic errors and determine which were statistically significant at a single wavelength, the regression was performed in a stepwise fashion.[5] It is emphasized that the errors at this stage were diagnosed as functions of true reflectance factor. The t-values and p-values were considered to test the Hypothesis: $\beta_m(\lambda)$= 0 at the 0.05 level of significance. The stepwise regression was repeated for several combinations of imaging system calibration target and spectrophotometric diagnostic targets. The five targets were used in the diagnostic process as spectrophotometric diagnostic targets. The photometric zero error, equal to the intercept of the regression equation, was always included in each regression. The frequency of the significant systematic errors at different wavelengths was calculated, plotted in Figure 1. In order to calculate the frequency of each systematic error, the t-values for each error and each case of imaging system calibration and spectrophotometric diagnostic targets were plotted against wavelength. Figure 2 shows the photometric nonlinear scale, $\beta_2(\lambda)$, as a function of wavelength for the case of having the Color Checker DC as the imaging system calibration target and Gamblin as the spectrophotometric diagnostic target. A significant diagnostic coefficient had $|t|>t_{\alpha/2}$ or $p<\alpha$ (α=0.05). The $t_{\alpha/2}$ and α=0.05 are shown by the green line in Figure 2. The significant coefficients at each case were found and added to calculate the frequency of the specific coefficient for the entire system.

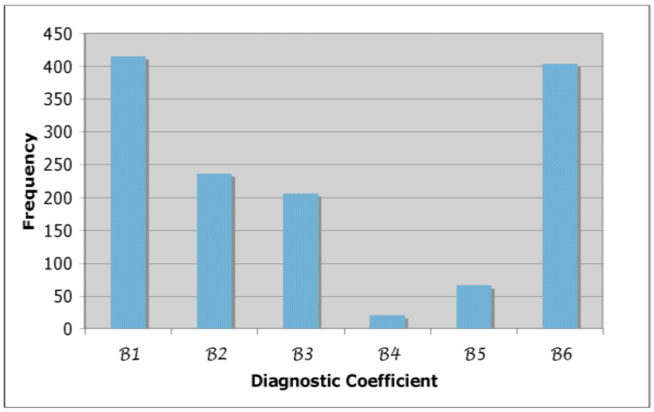

Figure 1. Frequency of significant diagnostic coefficients as a function of wavelength using different imaging system calibration and spectrophotometric diagnostic targets.

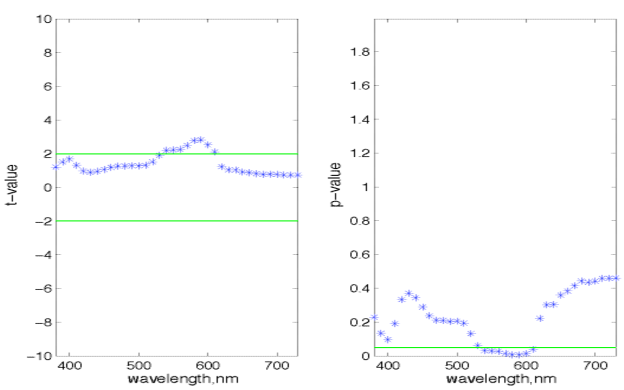

Figure 2. From left to right, t-value and p-value against wavelength for photometric nonlinear scale, $\beta 2$, for the case of Color Checker DC as the imaging system calibration target and Gamblin as the spectrophotometric diagnostic target. The green lines corresponds to $t\alpha/2$ and α=0.05 values.

It can be seen from Figure 1 that wavelength nonlinear scale error (quadratic, β_4) was less frequent in the imaging system. The most frequent errors were photometric linear scale, β_1, and bandwidth errors, β_6. Based on these statistical results it was concluded that the photometric zero, photometric linear scale, wavelength linear scale, and bandwidth could be the possible systematic errors in the spectral imaging system.

The diagnostic regression coefficients as a function of wavelength for the case of the Color Checker DC as the imaging system calibration target and Gamblin as the spectrophotometric diagnostic target are plotted in Figure 3. The photometric zero error is noticeable in all wavelengths. At wavelengths above 600 nm this error gets larger. The spectral variation of the photometric linear scale error is negligible. The curve shape of the wavelength linear scale suggests that the error at short and long wavelengths is larger than the middle portion of the spectrum. The shape of the bandwidth error supports the results of the stepwise regression, which identified the bandwidth error as a highly frequent error in the imaging system. Variation at different regions of the spectrum suggests that bandwidth error should be included in the regression model. The same trends were seen using different imaging system calibration and spectrophotometric diagnostic targets.

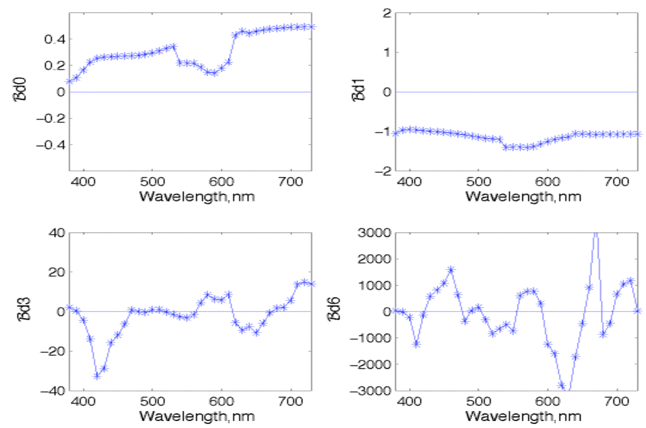

Figure 3. The diagnostic regression coefficients as a function of wavelength for the case of Color Checker DC as the imaging system calibration target and Gamblin as the spectrophotometric diagnostic target. $\beta d0$ represents the photometric zero error, $\beta d1$ represents the photometric linear scale error, $\beta d3$ represents the wavelength linear scale, and $\beta d6$ represents the bandwidth error.

The regression technique was implemented for correcting the estimated reflectance factor of different cases of imaging system calibration and spectrophotometric correction targets. Four error parameters were modeled: the photometric zero, the photometric linear scale, the wavelength linear scale, and the bandwidth. The effectiveness of this model was evaluated spectrally and colorimetrically. At this stage the systematic error was evaluated as a function of estimated reflectance factor. The analysis was extended using the estimated regression coefficients to correct the estimated reflectance factor data via Eq. 13. The differences between the "true" reflectance factor and the corrected reflectance factor for each spectrophotometric correction targets were evaluated. The effectiveness of the multiple linear regression on the spectral and colorimetric performance of CCDC as the imaging system calibration target and different cases of spectrophotometric correction targets are listed in Table II and shown in Figure 4. The regression model as a function of wavelength improved the performance of the spectral imaging system to a noticeable level. The same evaluation was performed for the other cases, each target as the imaging system calibration target and the remaining targets as the spectrophotometric correction targets. The percent improvement of average performance of average %RMS and

ΔE_{00} based on 25 sets of imaging system calibration and spectrophotometric correction targets was 25.3% and 16.7%, respectively.

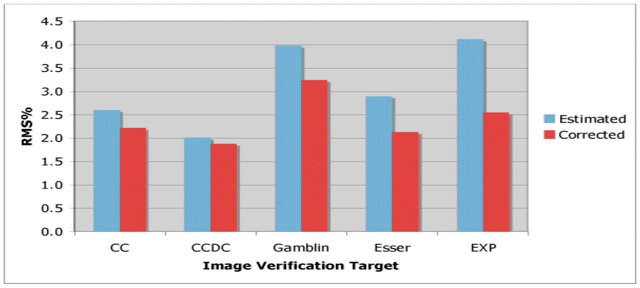

Figure 4. The average RMS% performance of the case of Color Checker DC as the imaging system calibration target and the others as the spectrophotometric correction targets.

Table 2: The Spectral RMS% and Colorimetric Performance of the Estimated Targets Based on Camera Model and Corrected Based on Regression Model. Color Checker DC is Imaging System Calibration Target

		RMS%		ΔE_{00}	
Spectroph. correction target		Estimated	Corrected	Estimated	Corrected
CC	mean	2.6	2.2	1.7	1.6
	max	9.3	6.4	2.8	4.6
CCDC	mean	2.0	1.9	1.6	1.6
	max	8.6	8.5	9.1	8.8
Gamblin	mean	4.0	3.2	2.3	2.2
	max	11.5	7.9	9.1	8.8
Esser	mean	2.9	2.1	2.2	1.3
	max	17.7	15.2	12.9	10.9
EXP	mean	4.1	2.6	2.1	1.2
	max	12.6	4.5	4.5	4.1

Different combinations of systematic errors were also employed to correct the estimated reflectance factor of Gamblin as the spectrophotometric correction target and CCDC as the imaging system calibration target. Figure 5 shows the colorimetric and spectral RMS% performance of the correction process. As it can be seen from Figure 5, in the case of considering the bandwidth error in the correction process, spectral performance was improved significantly. Figure 5 also supports the results of stepwise regression, which identified the bandwidth error as a highly frequent error in the imaging system.

Recall that the multiple linear regression was performed as a function of wavelength. The model fit was quantified by calculating the multiple correlation coefficient and consequently, the R-squared value. The R-squared is an overall indictor of regression fit and varies between 0 and 1 for poor and well-modeled data, respectively. R-squared as a function of wavelength is plotted in Figure 6 for each combination of imaging system calibration and spectrophotometric correction targets. The imaging system calibration targets are marked on each row of Figure 6 and spectrophotometric correction targets are shown in each column. In some cases, the data at short and long wavelengths were better fit than the data in the middle portion of the spectrum. In other cases, in which the both targets, imaging and spectrophotometric, were same, the data were modeled poorly. This means that the calibration procedure of the spectral imaging system functioned correctly. Again, the fitting of the data at short wavelengths is relatively high. This means that errors at short wavelengths are higher in these cases, which were expected. In the cases that the spectrophotometric correction target differs from imaging system calibration target, the regression technique was more successful to correct the imaging system. This issue is seen in the case of Gamblin and EXP as independent spectrophotometric correction targets.

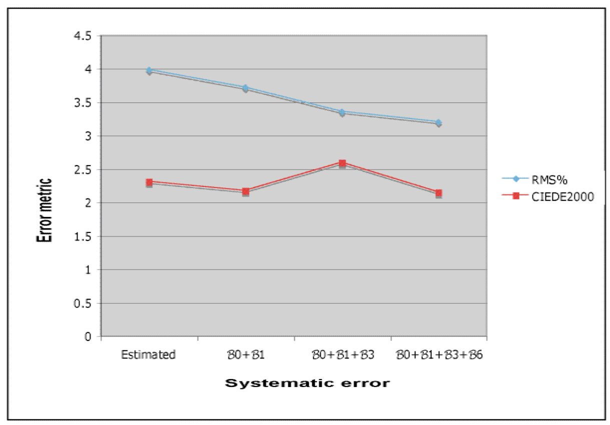

Figure 5. The average spectral RMS% and colorimetric performance of the case of Color Checker DC as the imaging system calibration target and the others as the spectrophotometric correction targets using different combination of systematic errors in correction process.

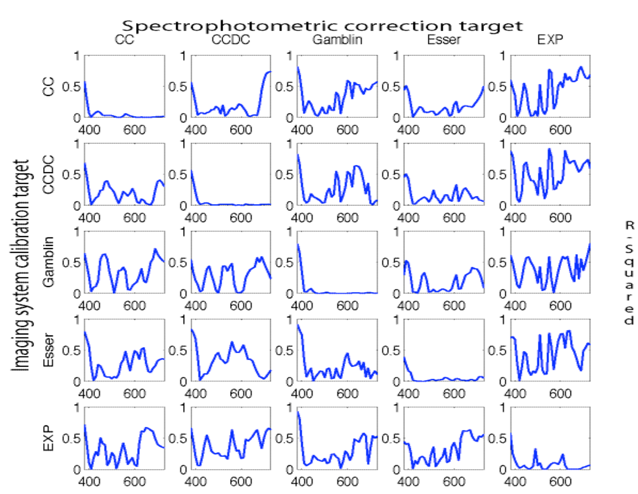

Figure 6. R-squared of multiple linear regression for correction of the estimated reflectance factor of the different spectrophotometric correction targets (columns) using different imaging system calibration targets (rows).

Conclusions

A technique based on multiple linear regression was described to diagnose and correct systematic errors in a spectral imaging system. The errors to diagnose were typical spectrophotometric errors and included photometric, wavelength, and bandwidth. Several sets of imaging system calibration and spectrophotometric targets were employed to both diagnose and correct systematic errors. The systematic errors were characterized as a function of wavelength. The diagnosed significant errors were photometric zero, photometric linear scale, wavelength linear scale, and bandwidth. The photometric zero errors were always included in the regression. This diagnostic process was helpful to figure out which systematic errors were most significant in the imaging system. That can lead one to adjust the imaging system operationally and mathematically. For example, a large photometric zero error is associated with stray light and flare in the imaging system, and it would be removed by controlling this parameter physically. The part of flare associated to the dark image (closed shutter of the digital camera) would be corrected using the current method. Also, differences in geometry of the imaging system calibration and spectrophotometric correction targets based on differences in surface reflection would contribute to the photometric errors and can be corrected using the proposed method.

The R-squared value as an index of regression fitting demonstrated that the imaging system performed well where the imaging system calibration and spectrophotometric correction targets were identical. In this case the multiple linear regression was not helpful to improve the system except in correcting the expected short wavelength errors. The effectiveness of the developed technique was demonstrated in correcting the independent spectro-photometric correction targets.

The estimated reflectance factors of the spectrophotometric correction targets were corrected using the developed technique. The average spectral %RMS and ΔE_{00} were improved 25.3% and 16.7%, respectively. The current technique is an indirect method to correct the transformation matrix derived based on SVD-based pseudo inverse technique. Since the transformation matrix is just a mathematical conversion from the captured digital count to the estimated reflectance factor, the systematic errors that might be included in an imaging system are not considered. Therefore, a correction model based on the idea of improving the accuracy of spectrophotometers can be applied to the spectral imaging. Since the transformation matrix and correction model was performed spectrally, the improvement of spectral performance of the total system was better than the colorimetric performance.

References

1. R. S. Berns, Billmeyer and Saltzman's Principle of Color Technology, 3rd edition, John Wiley & Sons, New York (2000).
2. R. S. Berns, K. H. Petersen, Empirical Modeling of Systematic Spectrophotometric Errors, Color Res. and Appl. 13, 243-256 (1988).
3. M. D. Fairchild, L. Reniff, Propagation of Random Errors in Spectrophotometric Colorimetry, Color Res. and Appl. 16, 360-367 (1991).
4. A.R. Robertson, Diagnostic Performance Evaluation of Spectrophotometers'' presented at Advances in Standards and Methodology in Spectrophotometry, Oxford, England, (1986).
5. R. A. Johnson, D. W. Wichern, Applied Multivariate Statistical Analysis, 5th edition, Prentice Hall, New Jersey (2002).
6. M. Mohammadi, M. Nezamabadi, L.A. Taplin, R. S. Berns, Pigment selection Using Kubelka-Munk Turbid Media Theory and Non-Negative Least Square Technique, MCSL Technical Report (2005).
7. M. Mohammadi, R. S. Berns, Verification of the Kubelka-Munk Turbid Media Theory for Artist Acrylic Paint, MCSL Technical Report, (2004).
8. M. Mohammadi, M. Nezamabadi, R. S. Berns, L.A. Taplin, Spectral Imaging Target Development Based on Hierarchical Cluster Analysis, in Proc. Of 12th Color Imaging Conference, 59-64 (2004).
9. M. Mohammadi, M. Nezamabadi, R. S. Berns, A Prototype Calibration Target for Spectral Imaging, in Proc. Of AIC Color 05, 387-390 (2005).
10. P. Kubelka, and F. Munk, 'Ein Beitrag Zur Optik der Farbanstriche', Zeitschrift fur technische Physik 12 593-601 (1931).
11. R. S. Berns, L.A. Taplin, M. Nezamabadi, Y. Zhao, Modification of a Sinarback 54 Digital Camera for Spectral and High-Accuracy Colorimetric Imaging: Simulations and Experimental, MCSl Technical Report (2004).

Acknowledgments

This research was supported by the Andrew W. Mellon Foundation, the National Gallery of Art, Washington, DC, the Museum of Modern Art, New York, and Rochester Institute of Technology, as part of the art spectral imaging project.

Author Biography

Mahnaz Mohammadi received her B.S. degree in Textile engineering from AmirKabir University at Tehran in 1993 and a M.S. in Polymer Engineering with an emphasis in color science from AmirKabir University in 1996. She worked for two years for Iran Color Research Center. Since 2002, she is a Ph.D. candidate in Imaging Science at the Munsell Color Science Laboratory of Rochester Institute of Technology.